Molecular BioSystems

PAPER

View Article Online
View Journal | View Issue

Cite this: *Mol. BioSyst.*, 2015, 11, 2786

Charting the interactome of PDE3A in human cells using an IBMX based chemical proteomics approach†

Eleonora Corradini,‡[ab] Gruson Klaasse,‡[c] Ulrike Leurs,§[a] Albert J. R. Heck,[ab] Nathaniel I. Martin*[c] and Arjen Scholten¶*[ab]

Received 19th February 2015,
Accepted 16th July 2015

DOI: 10.1039/c5mb00142k

www.rsc.org/molecularbiosystems

In the cell the second messenger cyclic nucleotides cAMP and cGMP mediate a wide variety of external signals. Both signaling molecules are degraded by the superfamily of phosphodiesterases (PDEs) consisting of more than 50 different isoforms. Several of these PDEs are implicated in disease processes inspiring the quest for and synthesis of selective PDE inhibitors, that unfortunately have led to very mixed successes in clinical trials. This may be partially caused by their pharmacological action. Accumulating data suggests that small differences between different PDE isoforms may already result in specific tissue distributions, cellular localization and different involvement in higher order signal protein complexes. The role of PDEs in these higher order signal protein complexes has only been marginally addressed, as no screening methodology is available to address this in a more comprehensive way. Affinity based chemical proteomics is a relatively new tool to identify specific protein–protein interactions. Here, to study the interactome of PDEs, we synthesized a broad spectrum PDE-capturing resin based on the non-selective PDE inhibitor 3-isobutyl-1-methylxanthine (IBMX). Chemical proteomics characterization of this resin in HeLa cell lysates led to the capture of several different PDEs. Combining the IBMX-resin with in-solution competition with the available more selective PDE inhibitors, cilostamide and papaverine, allowed us to selectively probe the interactome of PDE3A in HeLa cells. Besides known interactors such as the family of 14-3-3 proteins, PDE3A was found to associate with a PP2A complex composed of a regulatory, scaffold and catalytic subunit.

Introduction

Cellular communication is important for coordinating multitudinous activities between various cells and their extracellular environment. In mammalian cells, the cyclic nucleotides cAMP and cGMP are among the earliest identified signal transduction systems acting as mediators in transmitting a wide variety of external signals (Kim and Park, 2003 and Wang *et al.*, 2010). Although synthesis of cAMP and cGMP is carried out by entirely different enzymes, they are both degraded by the large superfamily of phosphodiesterases (PDEs).[1,2] The human genome encodes 21 PDE genes and thus far over 50 PDE isoforms categorized in 11 different families have been experimentally identified.[3] Given the complexity of the PDE family tree, it is now accepted that most of the different PDE variants are involved in specific physiological functions.[4] Many PDEs are reported to be localized along with other signaling proteins in so-called microdomains, allowing them to be strategically anchored throughout the cell.[5–7] In this regard, precise cellular compartmentalization of these enzymes allows control of cyclic nucleotide gradients and permits cAMP and cGMP specificity in space and time, but also the integration of cyclic nucleotide signaling with other pathways.[8]

PDEs have been implied in several disease processes, initiating the search for molecules with PDE inhibiting potential.[9] Naturally occurring methylxanthines, such as caffeine and theophylline were the first PDE-inhibitors to be discovered. These non-selective inhibitors, together with derivatives such as the 3-isobutyl-1-methylxanthine (IBMX (1), Fig. 1A), have been widely used as therapeutics. In particular, IBMX has been used to potentiate

[a] *Biomolecular Mass Spectrometry and Proteomics, Bijvoet Center for Biomolecular Research and Utrecht Institute for Pharmaceutical Sciences, Science Faculty, Utrecht University, Padualaan 8, 3584 CH Utrecht, The Netherlands. E-mail: ascholt1@its.jnj.com*

[b] *Netherlands Proteomics Centre, Padualaan 8, 3584 CH Utrecht, The Netherlands*

[c] *Department of Medicinal Chemistry and Chemical Biology, Utrecht Institute for Pharmaceutical Sciences, Utrecht University, Universiteitsweg 99, 3584 CG Utrecht, The Netherlands. E-mail: N.I.Martin@uu.nl*

† Electronic supplementary information (ESI) available: Supplemental Tables S1 and S2 and NMR data. See DOI: 10.1039/c5mb00142k

‡ These authors contributed equally to this work.

§ Current address: Department of Drug Design and Pharmacology, University of Copenhagen, Universitetsparken 2, 2100 Copenhagen, Denmark.

¶ Current address: Janssen, Infectious Diseases and Vaccines, Crucell Holland, Newtonweg 1, 2333 CP, Leiden, The Netherlands.

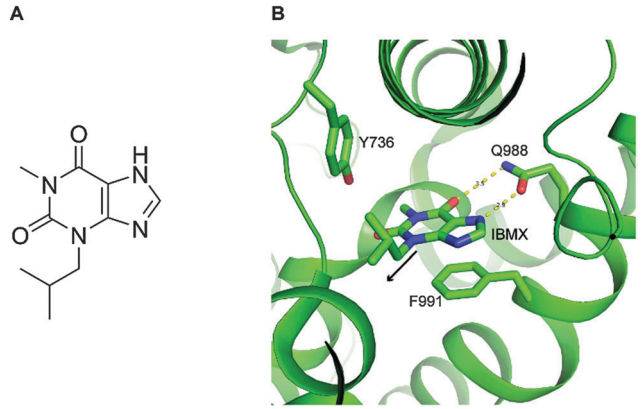

Fig. 1 (A) Structure of IBMX (1). (B) X-ray crystal structure of IBMX with PDE3B revealing the binding, but also the accessibility of the isobutyl group which points outwards along the black arrow. Oxygen atoms are shown in red and nitrogen atoms are in blue.

the effects of hormones that act *via* cAMP.[10] Later, more selective PDE inhibitors were synthetized[11] and applied as therapeutics for several diseases. For instance the PDE5 inhibitor, sildenafil was initially developed to treat pulmonary hypertension, however it has been approved as a drug to treat erectile dysfunction, since it displayed erectogenesis as a side effect. On the other hand PDE3 and PDE4 inhibitors were developed to treat cardiotonic, bronchodilatatory, vasodilatatory and anti-inflammatory activities. Unfortunately, their clinical use was not approved mainly due to intolerable side effects.[12,13]

These studies have taught us that generating PDE-inhibitors targeting a single PDE family branch with high potency is typically not sufficient. The reason for the reported side effects could also lie in the nature of the intracellular organization of PDEs. For instance, inhibiting a particular PDE-isoform localized at the cell membrane may induce the therapeutic effect while a subtly different splice isoform of the same PDE family localized at the ER may induce a side effect. Therefore, more information regarding cellular localization and interactomes has to be taken into account during the design of new protein inhibitors. To date, only a handful of PDE signaling nodes have been characterized in some detail. For example the complex of SERCA2, phospholambam, AKAP18 and the regulatory subunit of protein kinase A has been reported to interact with PDE3A in heart.[14]

Several methods have been developed for the identification of protein–protein interactions such as yeast two hybrid screens,[15,16] size exclusion chromatography,[17] sucrose gradient ultracentrifugation,[18] immunoprecipitation, and affinity purification of genetically tagged proteins.[19] Alternatively, several studies have proposed the use of small molecules such as activity based chemical probes,[20] inhibitors,[21,22] small peptides[23] and cyclic nucleotides[24] covalently linked to a resin for the isolation of specific enzyme classes and their higher order complexes. The combination of this enrichment technique with mass spectrometry and subsequent statistical and bioinformatics analysis is often termed chemical proteomics.

To chart the interactome of PDEs, here we set out to develop a quantitative, PDE-centric chemical proteomics approach. Therefore, the non-selective PDE inhibitor IBMX was modified to act as a specific PDE-bait. This broad PDE-capturing tool is combined with in solution competition with different more selective PDE inhibitors. Differential mass spectrometry analysis of such competed samples shows that the PP2A complex, composed by the PPP2CB catalytic subunit, the PPP2R1A scaffold subunit and the PPP2R2A regulatory subunit, binds in HeLa cells specifically to PDE3A, together with several of the known PDE3A interactors, *i.e.* the 14-3-3 proteins. Hence we expect that the application of our chemical proteomics method in different biological samples, using different specific competitive PDE inhibitors, will be a valuable approach for the identification of PDE containing signaling nodes.

Results and discussion

Design and synthesis of the immobilized IBMX-resin

To specifically capture PDEs and elucidate their interactomes we decided to make use of chemical proteomics. Although some PDEs can be efficiently captured using immobilized cyclic nucleotides, such approaches enrich primarily also for the kinases PKA and PKG and their interactors.[25] Therefore, we argued a more PDE-centric tool would be beneficial. Here we describe the design, synthesis and first application of such a chemical proteomics tool. The involvement of PDEs in several diseases made their catalytic site an attractive target for medicinal chemists. One of the first pharmacological tools to study PDEs was the molecule IBMX, a cyclic nucleotide competitive and non-selective inhibitor, synthetic derivative of the naturally occurring methylxanthines caffeine and theophylline. The exact inhibition mode of these compounds became more clear upon solving several crystal structures of isolated catalytic domains of human PDEs bound to IBMX.[26–29] All these structures show two common features: (I) the interaction of the planar xanthine ring forms a π–π electron-stacking interaction with a conserved phenylalanine in the catalytic sites and (II) the formation of a hydrogen bond with an invariant glutamine.[30] All the structures show that the isobutyl at the N3-position seems not to be essential for the binding of IBMX (Fig. 1B). Making use of these similar binding modes we decided to synthesize a linkable form of IBMX (IBMX-L, **10**) by substituting the isobutyl group with a hexylamine group, permitting covalent attachment of the molecule to a solid support *via* amide coupling.

The synthesis of IBMX-L **10** is illustrated in Fig. 2 and is based on previously described approaches for the preparation of substituted 1-methylxanthines.[31,32]

To begin, *p*-methoxybenzylamine was treated with triphosgene to generate the corresponding isocyanate which was directly treated with methylamine to yield asymmetric urea **2**. The urea was next heated with cyanoacetic acid followed by treatment with aqueous sodium hydroxide to generate the 6-amino uracil species **3**. Nitrosation of **3** was then performed by treatment with sodium nitrite in acetic acid after which dithionite reduction in aqueous ammonium hydroxide yielded the diamino intermediate **4**. Treatment of **4** with triethyl orthoformate at elevated temperature then led to formation

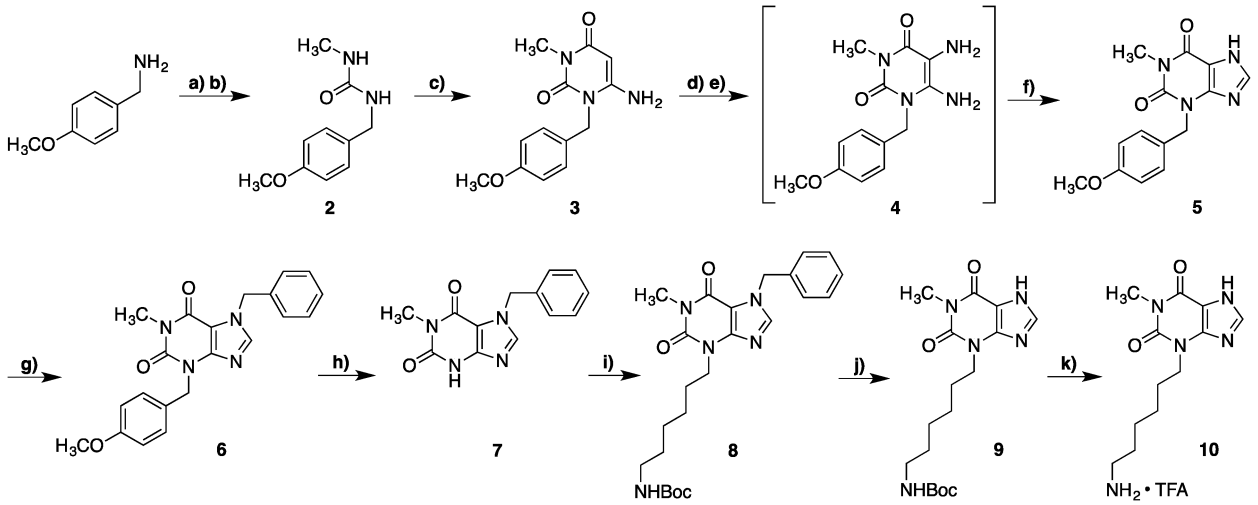

Fig. 2 Synthesis of linkable IBMX-L **10**. Reagents and conditions: (a) triphosgene, toluene, 115 °C; (b) 8 M $MeNH_2$ in EtOH, THF, 65 °C, 87% over 2 steps; (c) 1. Cyanoacetic acid, Ac_2O, 85 °C, 2. NaOH, H_2O, 79%; (d) $NaNO_2$, AcOH, 65 °C; (e) $Na_2S_2O_4$, NH_4OH, 50 °C, 53% over 2 steps; (f) $CH(OEt)_3$, EtOH, reflux, 83%; (g) B*n*Br, K_2CO_3, DMF, 35 °C, 76%; (h) TFA (neat), 105 °C, 90%; (i) *tert*-butyl (6-bromohexyl)carbamate, K_2CO_3, DMF, 65 °C, 78%; (j) PdO, H_2, MeOH, 95%; (k) TFA, CH_2Cl_2, 90%.

of intermediate **5** containing the intact xanthine core. Benzylation of the 7-position with benzyl bromide in DMF generated compound **6** after which the *p*-methoxybenzyl group at position 3 was removed by treatment with TFA to yield intermediate **7**. Alkylation of **7** with *tert*-butyl (6-bromohexyl)carbamate under basic conditions led to formation of compound **8** after which hydrogenation over palladium oxide cleanly removed the benzyl group to provide precursor **9**. Final Boc group removal with trifluoroacetic acid yielded the "linkable" IBMX-L species **10**. We could then form an amide bond between the IBMX-L and the *N*-hydroxy-succinimide (NHS) ester on NHS-activated agarose beads.

We resuspended the IBMX-L in anhydrous DMSO at a concentration of 100 mM, and incubated it at room temperature in darkness for 6 hours. IBMX exhibits IC_{50}s for mammalian PDEs that vary between 1 and 80 μM, except for PDE8 and PDE9 that do not bind substantially to IBMX ($IC_{50} > 100$ μM).[33] Therefore, in order to have a final concentration of the IBMX bound to the beads high enough to enrich a broad range of PDE families using a small volume of beads, we decided to immobilize IBMX with a final concentration of 6 μmol ml^{-1} of dried beads.

IBMX-resin affinity enrichment in HeLa cell lysates

After generating sufficient amounts of the IBMX-resin, we aimed to achieve the enrichment of endogenously expressed PDEs from a HeLa cell lysate (Fig. 3A). Whole cell extracts from HeLa cells were therefore incubated with the IBMX-resin. To confirm the specificity of the proteins that bound to the IBMX-resin we incubated the same amount of total protein lysate with NHS-activated beads blocked with ethanolamine. After incubation and washing, the proteins were eluted and separated on SDS-PAGE (Fig. 3B). Through digesting both gel lanes in 13 identical bands and subsequent analysis by LC-MS/MS (ESI,† Table S1), we identified 543 protein groups (see materials and methods for details on acceptance criteria) in the IBMX-resin lane and 516 proteins in the empty beads control. Previous studies have shown that phosphodiesterases are expressed in low abundance in HeLa cells.[34] Nevertheless PDE1A, PDE3A and PDE10A (Fig. 3C and ESI,† Table S1) showed a high enrichment with ample spectral counts in the IBMX-resin pull down, while they were completely absent in the pull down performed with the empty resin. This provides the first proof that the IBMX-resin can be used to enrich and identify several low abundant PDEs in a single experiment directly from a complex cell lysate. In order to evaluate the effectiveness of using the immobilized IBMX-L, as a ligand to enrich the PDEs under physiological conditions we measured and compared the IC_{50} for both IBMX and free IBMX-L for endogenous PDE3A binding to the IBMX-L resin from the HeLa cell lysate. Aliquots of HeLa cell extracts were incubated with both IBMX and IBMX-L at concentrations ranging from 50 nM to 500 μM and then probed with the same amount of IBMX-L resin. The resin eluates were separated on an SDS-PAGE, transferred to a PVDF membrane and then probed for PDE3A. In presence of the linker, IBMX-L shows an IC_{50} of 200 ± 50 μM, while IBMX shows an IC_{50} of 40 ± 25 μM (Fig. 3D). Although these *in vitro* measured IC_{50}s are not that low, we show that IBMX-L immobilized onto the beads allows for the efficient enrichment of the phosphodiesterases in our pull downs from cell lysates.

Competition with selective PDE inhibitors

Closer inspection of the data gathered from the in gel digestion already indicated the presence of a few known PDE3 interactors, members of the 14-3-3 family of proteins (ESI,† Table S1). In order to identify the exact interactome of PDE3A in HeLa cells, we further fine-tuned our method using specific PDE inhibitors to selectively compete single PDEs and their interactors off the broadly specific IBMX-resin. Cilostamide was described as the first potent selective inhibitor of PDE3 in platelets[35] with an IC_{50}

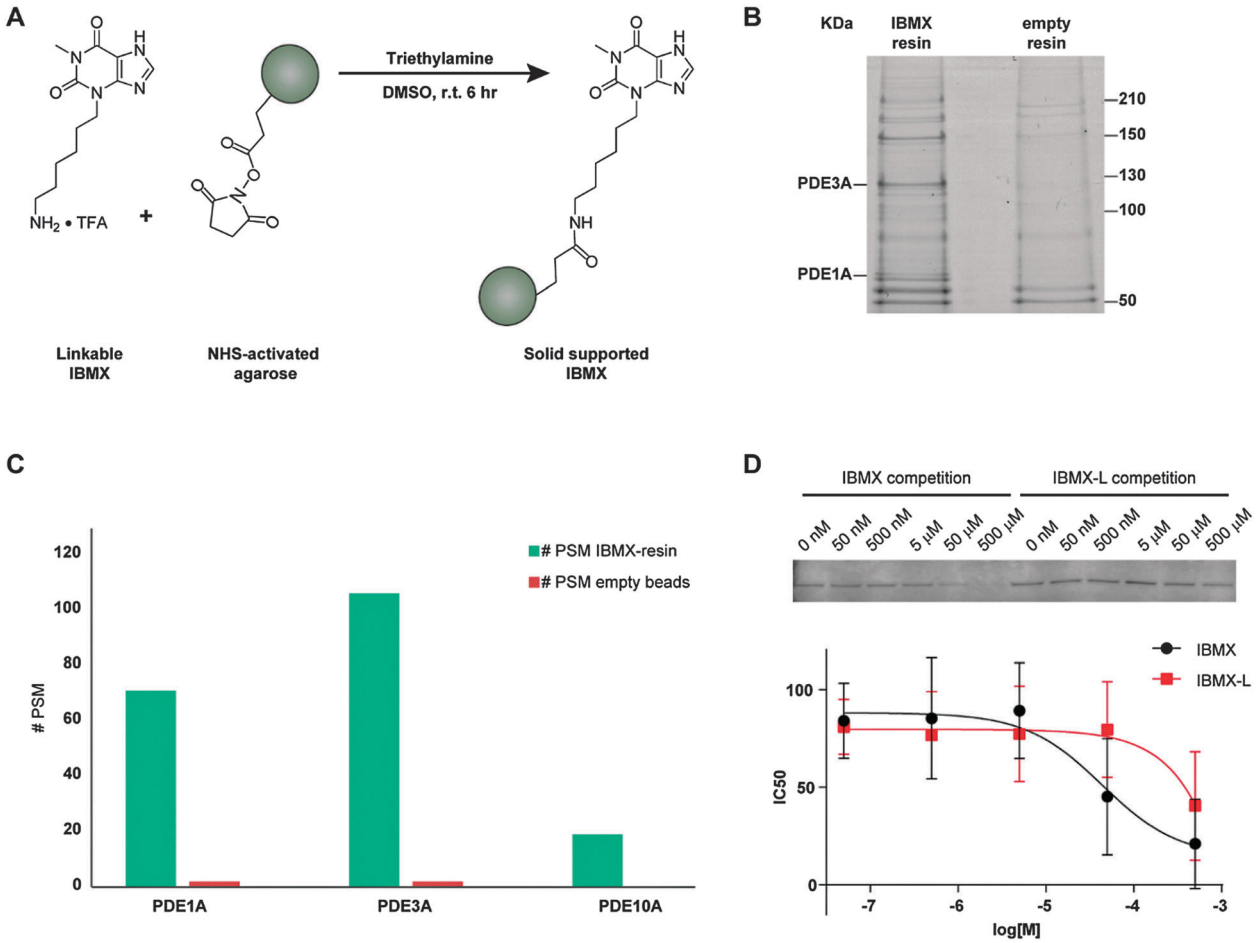

Fig. 3 Characterization of immobilized IBMX. (A) Immobilization of IBMX-L **(10)** on NHS-activated agarose beads. (B) Silver staining of the pull down performed in HeLa cells with IBMX-resin and NHS-agarose beads blocked with ethanolamine (control, empty beads). PDE3A and PDE1A were identified after in gel digestion and LC-MS/MS analysis (ESI,† Table S1). (C) Bar graph depicting the number of peptide spectral matches observed for each captured PDE in the gel lane of the IBMX-pull down and the pull down with the empty resin. PDE1A, PDE3A and PDE10A were highly enriched by the IBMX beads. (D) Western blot (n = 4) and thereof extracted IC_{50} profiles of IBMX and IBMX-L determined for PDE3A in the HeLa cell extract. The cell extracts were incubated with increasing amounts of inhibitors before the addition of IBMX-resin. Eluted proteins were separated on a SDS-PAGE and transferred to PVDF membrane. Western blots were performed in quadruplicate and probed for PDE3A.

of 70 nM. Papaverine is at present one of the most specific and selective inhibitors for PDE10A with an IC_{50} of 36 nM, however it also inhibits PDE3A *in vitro* with about an IC_{50} of 1.3 µM.[36] By using these two inhibitors, we could follow the affinity trend of both PDE isoforms in a single experiment. Hence, we performed two biological replicates in which three identical amounts of a HeLa lysate were incubated either with DMSO at a final concentration of 0.5% v/v (control), cilostamide (350 nM) or papaverine (250 nM). After the affinity enrichment, the three samples were digested, stable isotope labeled by using dimethyl labeling[37,38] and mixed in a 1 : 1 : 1 ratio. The DMSO treated control samples were labeled as light (L), the affinity enrichments supplemented with cilostamide were labeled as intermediate (M) and the affinity enrichments supplemented with papaverine were labeled as heavy (H). The peptides were analyzed *via* LC-MS/MS. The dimethyl ratios were evaluated using Proteome Discoverer whereby two biological replicates were compared. As expected, in both duplicates we identified PDE3A, PDE10A and PDE1A again. To assess the reproducibility of the pull downs we compared measured ratios in each biological replicate, *i.e.* cilostamide/control ratio from the biological replicate 1 *vs.* cilostamide/control ratio from the biological replicate 2 (Fig. 4A). When inspecting the cilostamide/control ratios, it is evident that the binding of PDE3A to the IBMX-resin was completely abolished showing an averaged M/L ratio for the two biological replicates of ~0.01. In contrast, PDE10A and PDE1A did not show any response towards cilostamide with ratios close to 1 (ESI,† Table S2A), indicating that adding cilostamide prevented only PDE3A to bind to the resins.

A different result was obtained upon competition with papaverine. The two biological replicates indicated that both PDE10A and PDE3A binding to the IBMX beads were nearly completely abolished by the addition of papaverine with respective averaged ratios of 0.1 and 0.01 (Fig. 4B).

On the other hand, PDE1A binding to IBMX was not affected by the presence of papaverine. *In vitro* measurements of papaverine's

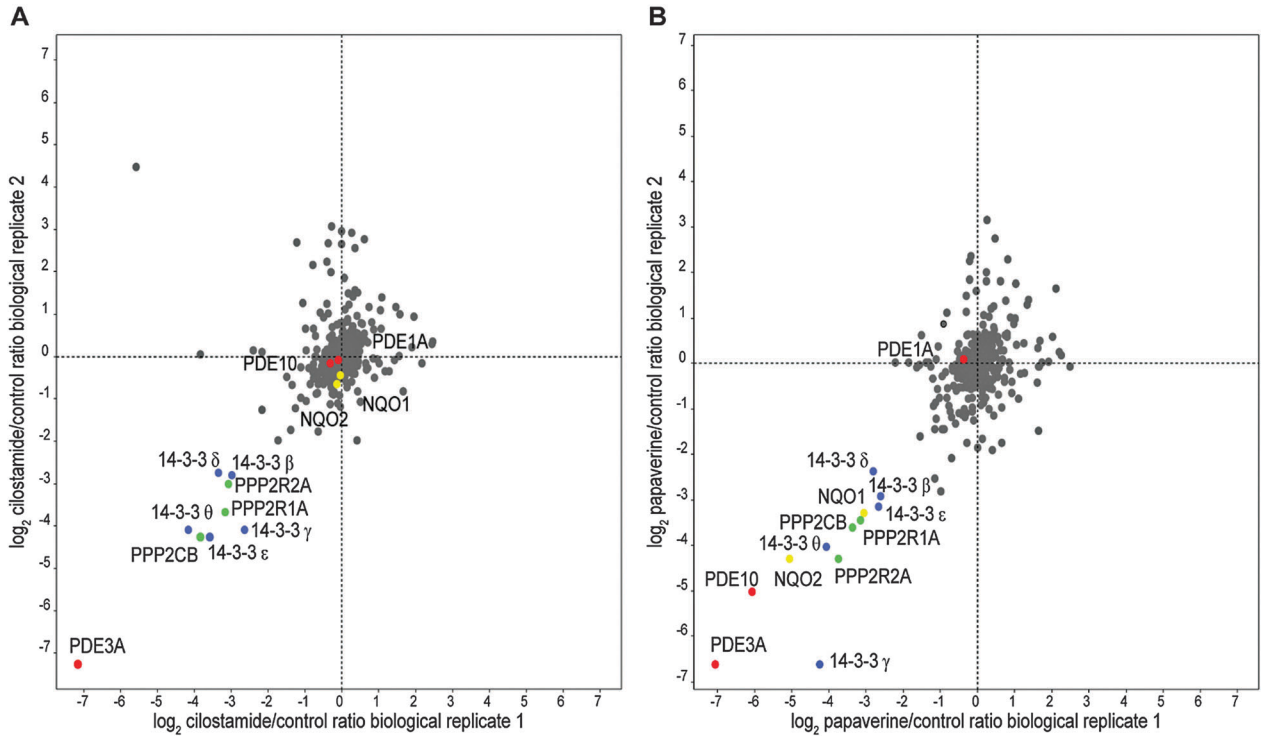

Fig. 4 Specifically enriched proteins following IBMX-based affinity enrichments in lysates supplemented with (A) cilostamide and (B) papaverine. The proteins of which the binding onto the beads is competed off by the presence of a specific PDE inhibitor in both biological replicates are localized at the bottom of the lower left quadrant. (A) Shows the correlation of the cilostamide/control ratios of the pull downs performed in two biological replicates. Proteins showing at least 2-fold lower enrichment in both biological replicates and at least two unique peptides were considered as possible PDE3A and PDE10A interactors. Upon competition with cilostamide, PDE3A binding to the beads is completely disrupted, while PDE10A and PDE1A remain at a ratio close to 1. In (B), are reported the papaverine/control ratios in the two biological replicates. After competition with papaverine, PDE3A and PDE10A binding to the beads is abolished, while the PDE1A ratio does not change. The proteins that do not show affinity for cilostamide or papaverine fall in the center of the plot with a ratio of ~1. The proteins that show a different trend in the two biological replicates were not considered for further analysis. Phosphodiesterases are shown in red, serine/threonine protein phosphatases in green, 14-3-3 proteins in blue, and putative PDE10A binding proteins in yellow.

IC_{50} for PDE3A, show a higher value when compared to the concentration we used in our experiments; 1.3 μM *vs.* 250 nM. We believe this may be explained by the different biological context where the measurements were performed in. Here, the effects of inhibitors were tested in a more physiological context, instead of with recombinant truncated PDEs *in vitro*. Therefore chemical proteomics approaches are an interesting tool to understand the mechanisms that take place during the PDEs inhibition and help in the design of even more specific PDE inhibitors.

Novel PDE3A interacting proteins

Competing with free cilostamide in solution did not only prevented PDE3A from binding to the beads, but also some other proteins were less enriched and maybe therefore be regarded as putative interactors (Fig. 4A, ESI,† Table S2A). The cilostamide competition *vs.* control (M/L) and the papaverine competition *vs.* control (H/L) ratios of these proteins were below 0.5 in both replicate experiments. We hypothesized that there are at least two different protein complexes that becomes less enriched following competitive binding using cilostamide. One of these consists of several 14-3-3 isoforms, which were shown to interact with PDE3A previously. Several studies showed that these proteins bind to PDE3A in response to its phosphorylation, while their interaction is completely disrupted after dephosphorylation of PDE3A.[39–41] Next to the 14-3-3 proteins we identified another complex that showed consistent lower enrichment, with the ratios of the samples competed with the inhibitors *vs.* the control below 0.5, in both biological replicates. This complex consisted of the β catalytic subunit of PP2A (PPP2CB), together with the α isoform of the scaffold subunit (PPP2R1A) and the α isoform of the regulatory subunit (PPP2R2A) (Fig. 4A).

We hypothesized that the binding with PP2A takes place in presence of cilostamide, for further inhibition of PDE3A. To confirm this hypothesis we performed co-immunoprecipitation of PDE3A in presence or absence of cilostamide. In gel digestion and subsequent mass spectrometric analysis of the gel lanes showed that, while the 14-3-3 proteins are present in both the experiments, the regulatory subunit of PP2A is present only when the immunoprecipitation is performed in the presence of cilostamide (Fig. 5A and ESI,† Table S2B). From these data we conclude that PP2A binding to PDE3A takes place after the inhibition of PDE3A *via* both, specific and non-specific inhibitors.

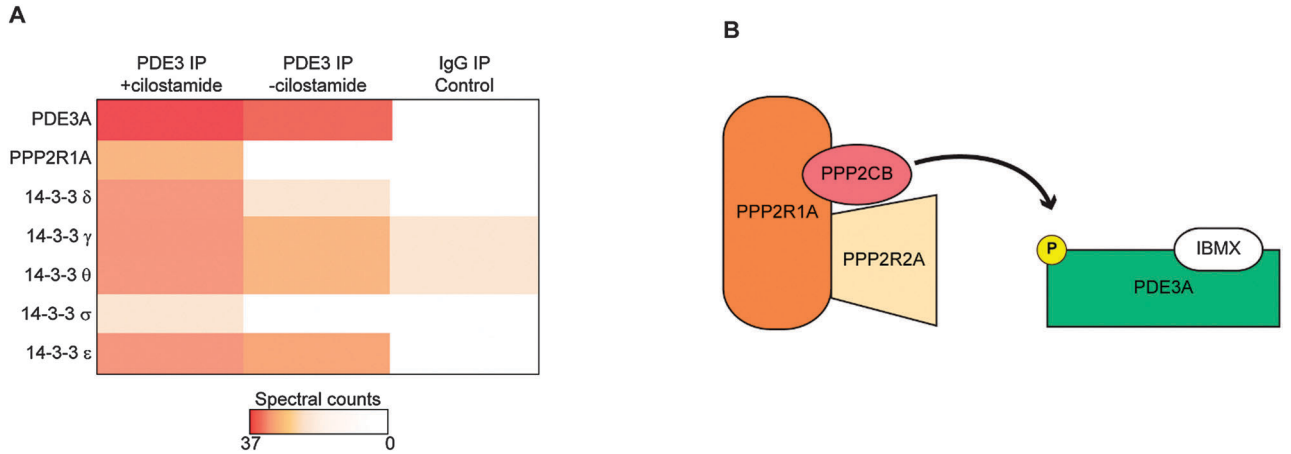

Fig. 5 (A) Spectral count heat map illustrating the interactome of PDE3A. Co-immunoprecipitation of PDE3A performed in presence of the competitive binder cilostamide reveal that PP2A regulatory subunits are co-purified, while the family of 14-3-3 proteins binds to PDE3A in both experiments. (B) Possible mechanism of interaction of PDE3A and PP2A after phosphodiesterase inhibition.

Upon competition with papaverine, not only PDE3A binding to the beads became less effective (Fig. 4B), also PDE10A showed a consistent H/L ratio around 0.01 in the two biological replicates. Together with PDE10A we also identified two other proteins displaying a H/L ratio below 0.5, the ribosyldihydronicotinamide dehydrogenase (NQO2) and the NAD(P)H dehydrogenase (NQO1). These two proteins show a high sequence homology and are known to bind to several small molecules, however they do not show similar specificity for the same inhibitors.[21,42] Both NQO1 and NQO2 were enriched in the IBMX-resin pull down, therefore we first hypothesized that they could be enriched by the resin itself (ESI,† Table S1). While both proteins were enriched in our control pull downs and the ones competed with 350 nM cilostamide, they were efficiently competed when papaverine was used as competitor. This suggested that these two proteins are likely interactors of PDE10A, since they show exactly the same competition behavior, *i.e.* captured by the resin, but competed by papaverine, but not cilostamide. However there is currently no evidence in the literature about these interactions and future follow up experiments are needed to confirm these results further.

In the last decade, through chemical proteomics based approaches a wide variety of small molecules, small peptides or activity based chemical probes have been used for the characterization of protein targets.[21,22,43] An extensive variety of PDE inhibitors have been synthetized in the past years due to the involvement of these proteins in several diseases, however only few of these inhibitors have been clinically approved, because of their side effects. Previous chemical proteomics studies based on the high affinity PDE5 inhibitor (PF-4540124) showed that together with PDE5, other proteins were targets of the inhibitor, giving the possibility to improve the binding of one of the other targets by derivatizing the small molecule.[44] In this work we used an opposite approach, where we derivatized the broad range inhibitor IBMX in order to link it to agarose beads and enrich for a variety of PDEs.

It has been suggested that also PDEs are assembled in an isoform-specific manner into specialized macromolecular complexes within discrete functional compartments, thereby allowing for precise spatiotemporal control of cyclic nucleotide signaling.[45,46] Therefore, we decided to use a competition with more selective inhibitors to identify possible interactors of enriched PDEs. With our method we were able to enrich for some of the low abundant isoforms of PDEs expressed in HeLa cell,[34] among which PDE1A, PDE3A and PDE10A showed the highest number of PSMs. In the past, particular attention has been directed towards PDE3 isoforms. For instance, analysis of signalosomes in cardiomyocytes suggested that upon phosphorylation PDE3A is incorporated into macromolecular regulatory complexes containing PDE3A, SERCA2, AKAP18 and the catalytic subunit of PP2A.[14] PDE3B, on the other hand has been extensively studied in adipocytes, where it has been found that its deactivation is dependent on dephosphorylation by PP2A, but not PP1,[47] however the direct interaction of PDE3A with the whole PP2A complex as observed in our study was not shown previously. Therefore we decided to follow up on PDE3A and confirm its interaction with PP2A.

PP2A is a heterotrimeric, evolutionary conserved serine/threonine phosphatase with regulatory functions in a wide range of cellular processes, including transcription, apoptosis, cell growth and cellular transformation.[48,49] The human genome encodes two catalytic subunits (PPP2CA, PPP2CB), two scaffolding subunits (PPP2R1A, PPP2R1B) and at least 15 known regulatory B subunits that, by combinatorial assembly, can potentially form a multitude of different trimeric PP2A complexes.[49,50] The versatile nature of this combinatorial subunit arrangement provides substrate specificity as well as temporal and spatial control of phosphatase activity. Glatter *et al.* described an elegant affinity-purification method for the identification of protein–protein interactions using the different subunits of PP2A as bait to study which PP2A complexes exist in human cells,[51] however in these studies PDE3A was not identified as a potential interactor. With our method we were able not only to identify known interactors of PDE3A, *i.e.* the 14-3-3 proteins, but also the PP2A complex composed by the same catalytic, regulatory and scaffold subunits in two biological replicates, confirming the validity of our

methodology for the identification of PDE interactors. By comparing the immunoprecipitation of PDE3A in presence or absence of cilostamide we show that PDE3A is binding to PP2A when it is inhibited (Fig. 5B). As final result, we can confirm the validity of our chemical proteomics method and the possible future application in tissue samples for the identification of novel PDE interactors.

Experimental

Materials

tert-Butyl (6-bromohexyl)carbamate was purchased from Sigma Aldrich. NHS-Activated agarose slurry was purchased from Pierce (Thermo Fisher Scientific). Anhydrous dimethylsulfoxid (DMSO), triethylamine (TEA), ethanolamine and cilostamide were purchased from Sigma Aldrich. Papaverine-HCl was purchased from Santa Cruz Biotechnology.

Synthetic procedures and analytical data

1-(4-Methoxybenzyl)-3-methylurea (2). To a solution of *p*-methoxybenzylamine (4.63 g, 34 mmol) in 400 ml of dry toluene was added triphosgene (15 g, 50 mmol). The resulting mixture was refluxed at 115 °C for 3.5 h. The volatiles were removed *in vacuo* and the residue was dissolved in 120 ml dry THF. An 8 M $MeNH_2$ solution in EtOH (12.5 ml, 100 mmol) was added and the mixture heated at 65 °C for 30 minutes. The reaction mixture was concentrated *in vacuo* and purified with column chromatography (silica gel, 230–400 mesh, Merck type 60) (95 : 5 DCM/MeOH) yielding a white solid (5.8 g, 87%). Analytical data: R_f 0.25 (95 : 5 DCM/MeOH); ^{1}H NMR (300 MHz, CD3OD) δ 7.18 (d, 2H), 6.84 (d, 2H), 4.22 (s, 2H), 3.75 (s, 3H) 2.69 (s, 3H); 13C NMR (75 MHz, CDCl3) δ 159.5, 158.7, 131.5, 128.6, 113.9, 55.2, 43.7, 26.9. HRMS (ESI) calcd for $C_{10}H_{15}N_2O_2$ $[M+H]^+$ 195.1132, found 195.1137.

6-Amino-1-(4-methoxybenzyl)-3-methylpyrimidine-2,4(1*H*,3*H*)-dione (3). Compound **2** (3.0 g, 15.4 mmol) was dissolved in 80 ml Ac2O. Cyanoacetic acid (3.0 g, 35.2 mmol) was added and the reaction mixture stirred at 85 °C for 2.5 h. A second (1 g, 11.7 mmol) and a third (0.5 g, 5.8 mmol) addition of cyanoacetic acid were each followed by another 30 minutes of stirring. The mixture was concentrated *in vacuo* and the residue treated with 20% NaOH solution. The aqueous layer was extracted with DCM (3 × 100 ml), the organic layers combined, dried, concentrated *in vacuo* and the product was purified with column chromatography (silica gel, 230–400 mesh, Merck type 60) (95 : 5 DCM/MeOH) yielding an off-white solid (3.2 g, 79%). Analytical data: R_f 0.25 (DCM : MeOH 95 : 5); ^{1}H NMR (300 MHz, CDCl3) δ n/a; 13C NMR (75 MHz, CDCl3) δ n/a; HRMS (ESI) calcd for $C_{13}H_{16}N_3O_3$ $[M+Na]^+$ 284.1006, found 284.1005.

3-(4-Methoxybenzyl)-1-methyl-1*H*-purine-2,6(3*H*,7*H*)-dione (5). To a suspension of compound **3** (3.2 g, 12 mmol) in H_2O (65 ml) and AcOH (3.5 ml) $NaNO_2$ (1 g, 14.5 mmol) was added and the reaction mixture was stirred for 2 h at 50 °C. Formation of a purple color indicated formation of the nitroso derivative. Additional $NaNO_2$ (1 g, 14.5 mmol) was added and the mixture stirred at 65 °C for another 2 h. Again additional $NaNO_2$ (300 mg, 4.3 mmol) was added and the reaction mixture stirred at 75 °C for 45 minutes. The reaction mixture was cooled to 0 °C on ice, the solids collected on a Buchner funnel and washed with cold water, followed by drying under vacuum overnight, yielding a purple solid (2.5 g, 72%) which was used in the next step without purification. To a suspension of the crude nitroso intermediate (2.5 g, 8.61 mmol) in 25% NH_4OH (50 ml) $Na_2S_2O_4$ (8.7 g, 50 mmol) was added and the reaction mixture stirred at 50 °C for 2.5 h. When the purple color had gradually disappeared, the reaction mixture was cooled to 0 °C and the solid that formed was collected on a Buchner funnel, washed with cold water, and dried under vacuum overnight yielding the diamino intermediate **4** as a light green solid (1.74 g 73%) that was used immediately in the next step without further purification. To a suspension of intermediate **4** (1.74 g, 6.3 mmol) in EtOH (30 ml) was added triethyl orthoformate (8.3 ml, 50 mmol) and the mixture refluxed for 6 h. After cooling, the mixture was concentrated *in vacuo* and the product directly isolated by column chromatography (95 : 5 DCM/MeOH) yielding compound **5** as an off-white solid (1.5 g, 83%). Analytical data: R_f 0.25 (95 : 5 DCM/MeOH); ^{1}H NMR (300 MHz, DMSO-d_6) δ 8.04 (s, 1H), 7.30 (d, 2H), 6.83 (d, 2H), 5.08 (s, 2H) 3.68 (s, 3H), 3.22 (s, 3H); ^{13}C NMR (75 MHz, DMSO-d_6) δ 159.0, 154.8, 151.4, 147.9, 141.0, 129.8, 129.3, 114.1, 106.9, 55.4, 49.0, 46.0, 28.2; HRMS (ESI) calcd for $C_{14}H_{15}N_4O_3$ $[M+H]^+$ 287.1144, found 287.1120.

7-Benzyl-3-(4-methoxybenzyl)-1-methyl-1*H*-purine-2,6(3*H*,7*H*)-dione (6). Compound **5** (1 g, 3.5 mmol) was dissolved in 10 ml dry DMF. K_2CO_3 (0.74 g, 5.3 mmol) and benzyl bromide (0.65 ml, 5.3 mmol) were added after which the reaction mixture stirred at 35 °C for 16 h. Water (10 ml) was added and after cooling to R.T. the product precipitated out of solution. After cooling on ice, the solids were collected on a glass filter funnel, dried under vacuum and purified by column chromatography (silica gel, 230–400 mesh, Merck type 60) (1 : 1 to 3 : 1 EtOAc/hexanes) yielding the desired compound in pure form as off-white crystals (1.01 g, 76%). Analytical data: R_f 0.4 (3 : 1 EtOAc/hexanes); ^{1}H NMR (300 MHz, $CDCl_3$) δ 7.57 (s, 1H), 7.48 (d, 2H), 7.34 (s, 5H), 6.82 (d, 2H), 5.48 (s, 2H), 5.21 (s, 2H), 3.76 (s, 3H), 3.39 (s, 3H); ^{13}C NMR (75 MHz, $CDCl_3$) δ 154.8, 150.5, 146.1, 139.9, 134.0, 128.1, 127.8, 127.1, 105.9, 49.3, 26.4; HRMS (ESI) calcd for $C_{21}H_{21}N_4O_3$ $[M+H]^+$ 377.1614, found 377.1584.

7-Benzyl-1-methyl-1*H*-purine-2,6(3*H*,7*H*)-dione (7). Compound **6** (300 mg, 80 mmol) was dissolved in 10 ml TFA and stirred overnight in a sealed high-pressure tube at 105 °C. The reaction mixture was cooled to R.T., concentrated *in vacuo* and the product isolated by column chromatography (silica gel, 230–400 mesh, Merck type 60) (95 : 5 DCM/MeOH) yielding compound **7** a white solid (191 mg, 90%). Analytical data: R_f 0.5 (95 : 5 DCM/MeOH); ^{1}H NMR (300 MHz, $CDCl_3$) δ 10.91 (s, 1H), 7.63 (s, 1H), 7.36 (s, 5H), 5.50 (s, 2H), 3.40 (s, 3H); ^{13}C NMR (75 MHz, $CDCl_3$) δ 154.8, 150.5, 146.1, 139.9, 134.0, 128.1, 127.8, 127.1, 105.9, 49.3, 26.4. HRMS (ESI) calcd for $C_{13}H_{13}N_4O_2$ $[M+H]^+$ 257.1039, found 257.1029.

***tert*-Butyl (6-(7-benzyl-1-methyl-2,6-dioxo-1*H*-purin-3(2*H*,6*H*,7*H*)-yl)hexyl)carbamate (8).** To a solution of compound **7** (100 mg,

0.39 mmol) in 10 ml dry DMF, K_2CO_3 (69 mg, 0.5 mmol) and *tert*-butyl (6-bromohexyl)carbamate (140 mg, 0.5 mmol) were added. The reaction mixture was stirred at 60 °C for 16 h, concentrated *in vacuo*, redissolved in DCM, washed with 20 ml H_2O, and the organic layer dried with Na_2SO_4. After solvent removal under vacuum the desired product was isolated by column chromatography (95 : 5 DCM/MeOH) yielding **8** as a colorless oil which crystallized upon standing (140 mg, 78%). Analytical data: R_f 0.3 (95 : 5 DCM/MeOH); ^{1}H NMR (300 MHz, $CDCl_3$) δ 7.55 (s, 1H), 7.35 (m, 5H), 5.48 (s, 2H), 4.07 (t, 2H) 3.38 (s, 3H), 3.07 (d, 2H), 1.74 (t, 2H), 1.41 (m, 15H); ^{13}C NMR (75 MHz, $CDCl_3$) δ 155.9, 155.3, 151.3, 148.6, 140.8, 135.3, 129.1, 128.6, 128.1, 107.0, 50.3, 43.4, 40.4, 29.8, 28.4, 28.0, 27.9, 26.3, 26.2. HRMS (ESI) calcd for $C_{24}H_{34}N_5O_4$ $[M+H]^+$ 456.2611, found 456.2608.

***tert*-Butyl (6-(1-methyl-2,6-dioxo-1*H*-purin-3(2*H*,6*H*,7*H*)-yl)hexyl)-carbamate (9).** Compound **8** (290 mg, 0.63 mmol) was dissolved in 10 ml dry MeOH. $PdO{\cdot}H_2O$ (100 mg) was added and the reaction mixture was shaken in a Parr apparatus at an initial pressure of 50 PSI of H_2 for 72 h. Shorter reaction times resulted in incomplete conversion. The catalyst was removed by filtration over celite and the filtrate concentrated *in vacuo*, yielding white crystals (220 mg, 95%). Analytical data: R_f 0.1 (90 : 10 DCM/MeOH); ^{1}H NMR (300 MHz, CD_3OD) δ 7.81 (s, 1H), 4.07 (t, 2H), 3.36 (s, 3H), 3.01 (t, 2H), 1.75 (t, 2H), 1.42 (15H); ^{13}C NMR (75 MHz, $CDCl_3$) δ 157.1, 155.8, 151.7, 147.9, 141.5, 108.8, 78.3, 43.4, 39.8, 29.4, 27.6, 27.4, 27.0, 26.1, 25.9; HRMS (ESI) calcd for $C_{17}H_{27}N_5O_4$ $[M+H]^+$ 366.2141, found 366.2147.

3-(6-Aminohexyl)-1-methyl-1*H*-purine-2,6(3*H*,7*H*)-dione (10, IBMX-L(inkable)). Compound **9** (220 mg, 0.6 mmol) was dissolved in 20 ml dry DCM and 20 ml TFA was added. The reaction mixture was stirred at R.T. for 1.5 h, after which thin layer chromatography indicated complete deprotection. The mixture was concentrated *in vacuo* and lyophilized to yield the product as a colorless glass/oil (204 mg, 90%). Analytical data: ^{1}H NMR (300 MHz, D_2O) δ 7.9 (s, 1H), 3.79 (t, 2H) 3.11 (s, 3H) 2.78 (t, 2H) 1.45 (m, 4H), 1.18 (m, 4H); ^{13}C NMR (75 MHz, D_2O) δ 155.6, 151.8, 145.9, 140.21, 118.0, 114.2, 107.1, 44.0, 39.2, 28.0, 26.9, 26.4, 25.1; HRMS (ESI) calcd for $C_{12}H_{20}N_5O_2$ $[M+H]^+$ 266.1617 found 266.1602.

Preparation of IBMX-resin

10 ml of NHS-activated agarose 50% slurry was equilibrated in 3 × 5 ml of anhydrous DMSO. The 5 ml of equilibrated beads were incubated with IBMX-L (**10**, 100 mM in anhydrous DMSO) to achieve a final coupled concentration of 6 μmol IBMX-L ml^{-1} of dry beads. The mixture was supplemented with 90 μl of 100% TEA, used as base for the formation of the amide bond and incubated at room temperature on an end-over-end shaker, for 6 hours in the dark. Coupling efficiency was determined by measuring 5 μl of the supernatant at different time points by UV-HPLC (Shimadzu LC-10ADvp equipped with a Zorbax Eclipse Plus C18, 2.1 × 50 mm, 1.8 μm, Agilent, λ = 289 nm). After IBMX-L coupling with a final density on the beads of 6 μmol ml^{-1} of beads, the non-reacted NHS-groups were blocked by incubation with 1.2 ml of 98% ethanolamine at room temperature on the end-over-end shaker overnight. In parallel, the active sites of 5 ml of dry NHS-activated agarose beads were blocked with 1.2 ml of ethanolamine, following the same procedure, to subsequently use the beads as negative control, later referred to as empty beads. After blocking the NHS-groups, the beads were washed with 3 × 10 ml of PBS and stored in PBS with 0.1% NaN_3 at 4 °C in a 25% slurry.

Cell culture

HeLa cells were grown to 80% confluence at 37° with 5% CO_2 in Dulbecco's modified Eagle's medium containing 10% of fetal bovine serum (Lonza) and 0.1% Pen/Strep (Lonza). After harvesting with trypsin, cells were washed in PBS, snap frozen in liquid nitrogen and kept at −80 °C until further use.

Sample preparation and pull down assay

1 × 10^8 HeLa cells were subjected to dounce homogenization on ice in 5 ml of PBS, 0.2% Tween-20 containing protease (Complete mini EDTA-free mixture, Roche Applied Science) and phosphatase inhibitors (PhosSTOP, Roche Applied Science). After centrifugation (20 000 × *g* for 10 min at 4 °C), the protein concentration of the supernatant was measured using the Bradford assay. 12 mg of proteins were incubated for 2.5 h either with 240 μL of dry IBMX-resin or empty beads as a control. Samples were eluted with Laemmli sample buffer and proteins were separated on a 4–12% bis-tris gradient gel. Gel lanes were digested according to standard procedure[52] by cutting 13 bands from each entire gel lane. Peptides were extracted from the gel bands with acetonitrile and dried *in vacuo* before LC-MS/MS analysis on an Orbitrap Elite.

For the experiments including in-solution competition, 12 mg of HeLa protein lysate, was either incubated with 350 nM cilostamide, 250 nM papaverine or DMSO (Control) at 4 °C for 30 minutes on an end-over-end shaker. The samples were subsequently incubated with 240 μL of dried IBMX-resin for 2.5 hours. Samples were then subjected to washes with 3 × 1 ml of PBS 0.1% Tween-20 for the control or with washing buffer supplemented with either cilostamide 350 nM or papaverine 250 nM. Bound proteins where then washed with 3 × 1 ml of PBS before elution. Proteins were eluted at 95 °C with 300 μL of a solution containing 2% SDS and 50 mM DTT. The volume was reduced to 30 μL using a 3 kDa cut off centrifugation filter (Millipore). 7 μl of Laemmli sample buffer 4× (Biorad) was added to the eluted proteins and incubated at 95 °C for 5 minutes. Samples were then run into a 4–12% bis-tris gradient gel (Bio-Rad) for about 1 cm to concentrate the sample prior to in-gel tryptic digestion. In-gel trypsin digestion was performed according to standard procedures. After digestion the peptides were concentrated and desalted, using an OASIS solid phase extraction plate (Waters). Subsequently in solution dimethyl labeling was performed.[37,38] Peptides originating from the control sample were labeled as light (L), while the pull downs competed with cilostamide and papaverine were labeled as intermediate (M) and heavy (H) respectively. Samples were mixed in a 1 : 1 : 1 ratio prior LC-MS/MS analysis on an Orbitrap QExactive.

Dose response curve and IC_{50} calculation

Pull downs were performed in presence of increasing concentrations of IBMX or IBMX-L ranging from 50 nM to 500 μM. Control pull downs were performed in the absence of the inhibitor. Briefly, 500 μg of protein extract was incubated with the inhibitors at 4 °C for 30 minutes. The samples were subsequently incubated with 20 μl of dried IBMX-resin for 2.5 hours. After washes with PBS 0.1% tween-20 the proteins were eluted and separated on a 4–12% bis-tris gradient gel (Bio-Rad). The proteins were then transferred on a PVDF membrane and probed for PDE3A (abcam, ab99236, dilution 1 : 2000). After several washes the blots were incubated with Cy5 labeled secondary antibody (GE Healthcare) and detection was performed on a Typhoon 9400 imager (GE Healthcare). Quantitation was performed with Image Quant TL. Four biological replicates were performed and curves were fitted to the average values, while the top of the curve was fixed to 100 (empty control).

PDE3A co-immunoprecipitation

Cultured HeLa cells were lysed with a dounce homogenizer in lysis buffer (50 mM Tris-HCl (pH 8), 150 mM NaCl and 0.5% triton) in the presence of phosphatase inhibitors and protease inhibitors. 400 μg of proteins were diluted in 500 μl of lysis buffer and subsequently incubated for 3 h with 4 μg of PDE3A antibody (abcam, ab99236) at 4 °C, in presence or absence of 350 nM cilostamide. 20 μl of protein A magnetic beads slurry (Life Technologies) were added to the samples and incubated overnight at 4 °C. Samples were then washed with 3 × 400 μl washing buffer (50 mM Tris-HCl (pH 8), 150 mM NaCl and 0.05% triton). A parallel immunoprecipitation using rabbit IgG was performed as negative control following the same procedure. Samples were eluted with Laemmli sample buffer and proteins were separated on a 4–12% bis-tris gradient gel. The gel lanes were divided in 5 parts and subjected to trypsin digestion as described above. Extracted peptides were analyzed on a TripleTOF 5600 (AB Sciex, Concord, ON, Canada) mass spectrometer.

NanoLC-MS/MS

Pull downs performed with IBMX-resin and empty beads were analyzed on an Orbitrap Elite mass spectrometer (Thermo Scientific, San Jose, CA), IBMX pull downs performed in presence of cilostamide and papaverine were analyzed on a Q-Exactive both coupled to a Proxeon Easy-nLC 1000 (Thermo Scientific, Odense, Denmark), while the PDE3A IP were analyzed on a TripleTOF 5600 (AB Sciex, Concord, ON, Canada) coupled to an Agilent 1290 Infinity System (Agilent Technologies, Palo Alto, CA).

After reconstitution in 10% FA, 5% dimethyl sulfoxide, the peptides were separated on an in-house made 50 cm column with a 50 μm inner diameter packed with 2.7 μm C18 resin (Poroshell, Agilent Technologies Palo Alto, CA) operated at a constant temperature of 40 °C. The column was connected to the mass spectrometer through a nanoelectrospray ion source. The injected peptides were first trapped with a double fritted trapping column (Dr Maisch Reprosil C18, 3 μm, 2 cm × 100 μm) at a pressure of 600 bar with 100% solvent A (0.1% formic acid in water) before being chromatographically separated by a linear gradient of buffer B (0.1% formic acid in acetonitrile) from 7% up to 30% in 35 or 150 min (for the in-gel digested bands or for the whole pull downs respectively) at a flow rate of 100 nl min^{-1}.

Nanospray was achieved with an in-house pulled and gold-coated fused silica capillary (360 μm outer diameter, 20 μm inner diameter, 10 μm tip inner diameter) and an applied voltage of 1.7 kV. Full-scan MS spectra (from m/z 350 to 1500) were acquired in the Orbitrap with a resolution of 35 000 for the Q-Exactive and 30 000 for the Orbitrap Elite. Up to ten most intense ions above the threshold of 500 counts were selected for fragmentation. HCD fragmentation was performed when using the Q-Exactive with a data dependent mode, as previously described.[53] RapidCID was performed when using the Orbitrap Elite as described before.[54]

For the TripleTOF 5600 a voltage of 2.7 kV was applied to the needle. The survey scan was from 350 to 1250 m/z and the high resolution mode was utilized, reaching a resolution of up to 40 000. Tandem mass spectra were acquired in high sensitivity mode with a resolution of 20 000. The 10 most intense precursors were selected for subsequent fragmentation using an information dependent acquisition, with a minimum acquisition time of 100 ms.

Data analysis

The raw files collected from the TripleTOF were first recalibrated based on two background ions with m/z values of 371.1012 and 445.1200. The calibrated raw files were converted to mgf by the AB Sciex MS Data Converter (version 1.1 beta) program.

Peak lists were generated using Proteome Discoverer (version 1.4, Thermo Scientific, Bremen, Germany) for the raw files obtained from the Orbitrap instruments and for the mgf files generated from the AB Sciex program using a standardized workflow. Peak lists, were searched against a Swiss-Prot database (taxonomy human, 20 407 protein entries) supplemented with frequently observed contaminants, using Mascot (version 2.4 Matrix Science, London, UK). The database search was performed using the following parameters: a mass tolerance of 50 ppm for the precursor masses and ±0.6 Da for CID fragment ions and ±0.05 or ±0.15 Da for HCD fragments for the files acquired on the Orbitrap or on the TripleTOF, respectively. Enzyme specificity was set to Trypsin with 2 missed cleavages allowed. Carbarmidomethylation of cysteines was set as fixed modification, oxidation of methionine, dimethyl labeling (L, I, H) of lysine residues and N termini (when dimethyl labeling was performed) were used as variable modifications. Percolator was used to filter the PSMs for <1% false discovery-rate. When applicable, triplex dimethyl labeling was used as quantification method, with a mass precision of 2 ppm for consecutive precursor mass scans. A retention time tolerance of 0.5 min was used to account for the potential retention time shifts due to deuterium. To further filter for high quality data we used the following parameters: high confidence peptide spectrum matches, minimal Mascot score

of 20, minimal peptide length of 6 and only unique rank 1 peptides. For the identification and quantitation of the proteins, only unique peptides were considered. Protein ratios were normalized based on the protein median. Proteins showing an on/off situation were manually quantified by giving them an arbitrary value of 100 or 0.01 for extreme up- or down-regulation, which corresponds to the maximum allowed fold change in the used Proteome Discoverer settings. The mass spectrometry proteomics data have been deposited to the ProteomeXchange Consortium[55] via the PRIDE partner repository with the dataset identifier PXD001781.

Conclusions

With the chemical proteomics method presented in this work we show that the use of a broad range PDE inhibitor such as IBMX, immobilized on agarose beads, in combination with in solution competition with specific PDE inhibitors is a powerful tool to screen for PDE interactors. This method can be applied in the future to any type of cell, but also directly to tissue lysates, to further screen for PDE complexes and identify new interactors at an endogenous level.

Acknowledgements

We would like to acknowledge Dr Weng Chuan Peng for his technical support on the use of PyMOL. This work was partly supported by the PRIME-XS project (grant agreement number 262067) funded by the European Union 7th Framework Programme. This work is also part of the project Proteins At Work, a program of the Netherlands Proteomics Centre financed by the Netherlands Organisation for Scientific Research (NWO) as part of the National Roadmap Large-scale Research Facilities of the Netherlands (project number 184.032.201).

Notes and references

1 T. Braumann, C. Erneux, G. Petridis, W. D. Stohrer and B. Jastorff, Hydrolysis of cyclic nucleotides by a purified cGMP-stimulated phosphodiesterase: structural requirements for hydrolysis, *Biochim. Biophys. Acta*, 1986, **871**, 199–206.

2 H. L. Trong, N. Beier, W. K. Sonnenburg, S. D. Stroop, K. A. Walsh, J. A. Beavo and H. Charbonneau, Amino acid sequence of the cyclic GMP stimulated cyclic nucleotide phosphodiesterase from bovine heart, *Biochemistry*, 1990, **29**, 10280–10288.

3 K. Omori and J. Kotera, Overview of PDEs and their regulation, *Circ. Res.*, 2007, **100**, 309–327.

4 A. T. Bender and J. A. Beavo, Cyclic nucleotide phosphodiesterases: molecular regulation to clinical use, *Pharmacol. Rev.*, 2006, **58**, 488–520.

5 M. D. Houslay and D. R. Adams, PDE4 cAMP phosphodiesterases: modular enzymes that orchestrate signalling cross-talk, desensitization and compartmentalization, *Biochem. J.*, 2003, **370**, 1–18.

6 J. D. Scott, Compartmentalized cAMP signalling: a personal perspective, *Biochem. Soc. Trans.*, 2006, **34**, 465–467.

7 D. M. F. Cooper, Compartmentalization of adenylate cyclase and cAMP signalling, *Biochem. Soc. Trans.*, 2005, **33**, 1319–1322.

8 G. S. Baillie, Compartmentalized signalling: spatial regulation of cAMP by the action of compartmentalized phosphodiesterases, *FEBS J.*, 2009, **276**, 1790–1799.

9 S. H. Francis, J. L. Busch, J. D. Corbin and D. Sibley, cGMP-dependent protein kinases and cGMP phosphodiesterases in nitric oxide and cGMP action, *Pharmacol. Rev.*, 2010, **62**, 525–563.

10 C. Schudt, A. Hatzelmann, R. Beume and H. Tenor, Phosphodiesterase inhibitors: history of pharmacology, *Handb. Exp. Pharmacol.*, 2011, 1–46.

11 T. R. Russell, W. L. Terasaki and M. M. Appleman, Separate phosphodiesterases for the hydrolysis of cyclic adenosine 3′,5′-monophosphate and cyclic guanosine 3′,5′-monophosphate in rat liver, *J. Biol. Chem.*, 1973, **248**, 1334–1340.

12 M. Movsesian, O. Wever-Pinzon and F. Vandeput, PDE3 inhibition in dilated cardiomyopathy, *Curr. Opin. Pharmacol.*, 2011, **11**, 707–713.

13 H. Tenor, A. Hatzelmann, R. Beume, G. Lahu, K. Zech and T. D. Bethke, Pharmacology, clinical efficacy, and tolerability of phosphodiesterase-4 inhibitors: impact of human pharmacokinetics, *Handb. Exp. Pharmacol.*, 2011, 85–119.

14 S. Beca, F. Ahmad, W. Shen, J. Liu, S. Makary, N. Polidovitch, J. Sun, S. Hockman, Y. W. Chung, M. Movsesian, E. Murphy, V. Manganiello and P. H. Backx, Phosphodiesterase type 3A regulates basal myocardial contractility through interacting with sarcoplasmic reticulum calcium ATPase type 2a signaling complexes in mouse heart, *Circ. Res.*, 2013, **112**, 289–297.

15 S. Fields and O. Song, A novel genetic system to detect protein–protein interactions, *Nature*, 1989, **340**, 245–246.

16 S. J. Yarwood, M. R. Steele, G. Scotland, M. D. Houslay and G. B. Bolger, The RACK1 signaling scaffold protein selectively interacts with the cAMP-specific phosphodiesterase PDE4D5 isoform, *J. Biol. Chem.*, 1999, **274**, 14909–14917.

17 A. R. Kristensen, J. Gsponer and L. J. Foster, A high-throughput approach for measuring temporal changes in the interactome, *Nat. Methods*, 2012, **9**, 907–909.

18 M. S. Lange, B. Müller and M. Ueffing, Native fractionation: isolation of native membrane-bound protein complexes from porcine rod outer segments using isopycnic density gradient centrifugation, *Methods Mol. Biol.*, 2008, **484**, 161–175.

19 J.-P. Lambert, G. Ivosev, A. L. Couzens, B. Larsen, M. Taipale, Z.-Y. Lin, Q. Zhong, S. Lindquist, M. Vidal, R. Aebersold, T. Pawson, R. Bonner, S. Tate and A.-C. Gingras, Mapping differential interactomes by affinity purification coupled with data-independent mass spectrometry acquisition, *Nat. Methods*, 2013, **10**, 1239–1245.

20 A. E. Speers and B. F. Cravatt, Chemical strategies for activity-based proteomics, *ChemBioChem*, 2004, **5**, 41–47.

21 M. Bantscheff, D. Eberhard, Y. Abraham, S. Bastuck, M. Boesche, S. Hobson, T. Mathieson, J. Perrin, M. Raida, C. Rau, V. Reader, G. Sweetman, A. Bauer, T. Bouwmeester,

C. Hopf, U. Kruse, G. Neubauer, N. Ramsden, J. Rick, B. Kuster and G. Drewes, Quantitative chemical proteomics reveals mechanisms of action of clinical ABL kinase inhibitors, *Nat. Biotechnol.*, 2007, **25**, 1035–1044.

22 J. Wissing, L. Jansch, M. Nimtz, G. Dieterich, R. Hornberger, G. Keri, J. Wehland and H. Daub, Proteomics analysis of protein kinases by target class-selective prefractionation and tandem mass spectrometry, *Mol. Cell. Proteomics*, 2007, **6**, 537–547.

23 M. Vermeulen, K. W. Mulder, S. Denissov, W. W. M. P. Pijnappel, F. M. A. van Schaik, R. A. Varier, M. P. A. Baltissen, H. G. Stunnenberg, M. Mann and H. T. M. Timmers, Selective anchoring of TFIID to nucleosomes by trimethylation of histone H3 lysine 4, *Cell*, 2007, **131**, 58–69.

24 A. Scholten, M. K. Poh, T. A. van Veen, B. van Breukelen, M. A. Vos and A. J. Heck, Analysis of the cGMP/cAMP interactome using a chemical proteomics approach in mammalian heart tissue validates sphingosine kinase type 1-interacting protein as a genuine and highly abundant AKAP, *J. Proteome Res.*, 2006, **5**, 1435–1447.

25 T. T. Aye, S. Soni, T. A. van Veen, M. A. van der Heyden, S. Cappadona, A. Varro, R. A. de Weger, N. de Jonge, M. A. Vos, A. J. Heck and A. Scholten, Reorganized PKA-AKAP associations in the failing human heart, *J. Mol. Cell. Cardiol.*, 2012, **52**, 511–518.

26 G. Scapin, S. B. Patel, C. Chung, J. P. Varnerin, S. D. Edmondson, A. Mastracchio, E. R. Parmee, S. B. Singh, J. W. Becker, L. H. T. Van der Ploeg and M. R. Tota, Crystal structure of human phosphodiesterase 3B: atomic basis for substrate and inhibitor specificity, *Biochemistry*, 2004, **43**, 6091–6100.

27 H. Wang, Y. Liu, Y. Chen, H. Robinson and H. Ke, Multiple elements jointly determine inhibitor selectivity of cyclic nucleotide phosphodiesterases 4 and 7, *J. Biol. Chem.*, 2005, **280**, 30949–30955.

28 H. Wang, Y. Liu, Q. Huai, J. Cai, R. Zoraghi, S. H. Francis, J. D. Corbin, H. Robinson, Z. Xin, G. Lin and H. Ke, Multiple conformations of phosphodiesterase-5: implications for enzyme function and drug development, *J. Biol. Chem.*, 2006, **281**, 21469–21479.

29 H. Wang, M. Ye, H. Robinson, S. H. Francis and H. Ke, Conformational variations of both phosphodiesterase-5 and inhibitors provide the structural basis for the physiological effects of vardenafil and sildenafil, *Mol. Pharmacol.*, 2008, **73**, 104–110.

30 H. Ke and H. Wang, Crystal structures of phosphodiesterases and implications on substrate specificity and inhibitor selectivity, *Curr. Top. Med. Chem.*, 2007, **7**, 391–403.

31 M. Merlos, L. Gomez, M. Vericat, J. Bartroli, J. Garcia-Rafanell and J. Forn, Structure–activity relationships in a series of xanthine derivatives with antibronchoconstrictory and bronchodilatory activities, *Eur. J. Med. Chem.*, 1990, **25**, 653–658.

32 R. A. Hartz, K. K. Nanda, C. L. Ingalls, V. T. Ahuja, T. F. Molski, G. Zhang, H. Wong, Y. Peng, M. Kelley, N. J. Lodge, R. Zaczek, P. J. Gilligan and G. L. Trainor, Design, synthesis, and biological evaluation of 1,2,3,7-tetrahydro-6h-purin-6-one and 3,7-dihydro-1h-purine-2,6-dione derivatives as corticotropin-releasing factor(1) receptor antagonists, *J. Med. Chem.*, 2004, **47**, 4741–4754.

33 G. D. K. F. Rabe, *Phosphodiesterase Inhibitors*, Elsevier, 1996, pp. 41–64.

34 T. Geiger, A. Wehner, C. Schaab, J. Cox and M. Mann, Comparative proteomic analysis of eleven common cell lines reveals ubiquitous but varying expression of most proteins, *Mol. Cell. Proteomics*, 2012, **11**, M111 014050.

35 H. Hidaka, H. Hayashi, H. Kohri, Y. Kimura, T. Hosokawa, T. Igawa and Y. Saitoh, Selective inhibitor of platelet cyclic adenosine monophosphate phosphodiesterase, cilostamide, inhibits platelet aggregation, *J. Pharmacol. Exp. Ther.*, 1979, **211**, 26–30.

36 J. A. Siuciak, D. S. Chapin, J. F. Harms, L. A. Lebel, S. A. McCarthy, L. Chambers, A. Shrikhande, S. Wong, F. S. Menniti and C. J. Schmidt, Inhibition of the striatum-enriched phosphodiesterase PDE10A: a novel approach to the treatment of psychosis, *Neuropharmacology*, 2006, **51**, 386–396.

37 P. J. Boersema, R. Raijmakers, S. Lemeer, S. Mohammed and A. J. Heck, Multiplex peptide stable isotope dimethyl labeling for quantitative proteomics, *Nat. Protoc.*, 2009, **4**, 484–494.

38 D. Kovanich, S. Cappadona, R. Raijmakers, S. Mohammed, A. Scholten and A. J. Heck, Applications of stable isotope dimethyl labeling in quantitative proteomics, *Anal. Bioanal. Chem.*, 2012, **404**, 991–1009.

39 M. Pozuelo Rubio, D. G. Campbell, N. A. Morrice and C. Mackintosh, Phosphodiesterase 3A binds to 14-3-3 proteins in response to PMA-induced phosphorylation of Ser428, *Biochem. J.*, 2005, **392**, 163–172.

40 M. Rubio, K. Geraghty, B. Wong, N. Wood, D. G. Campbell, N. A. Morrice and C. Mackintosh, 14-3-3-affinity purification of over 200 human phosphoproteins reveals new links to regulation of cellular metabolism, proliferation and trafficking, *Biochem. J.*, 2004, **379**, 395–408.

41 S. E. M. Meek, W. S. Lane and H. Piwnica-Worms, Comprehensive proteomic analysis of interphase and mitotic 14-3-3-binding proteins, *J. Biol. Chem.*, 2004, **279**, 32046–32054.

42 F. Vella, G. Ferry, P. Delagrange and J. A. Boutin, NRH: quinone reductase 2: an enzyme of surprises and mysteries, *Biochem. Pharmacol.*, 2005, **71**, 1–12.

43 C. M. Salisbury and B. F. Cravatt, Activity-based probes for proteomic profiling of histone deacetylase complexes, *Proc. Natl. Acad. Sci. U. S. A.*, 2007, **104**, 1171–1176.

44 P. Dadvar, M. O'Flaherty, A. Scholten, K. Rumpel and A. J. R. Heck, A chemical proteomics based enrichment technique targeting the interactome of the PDE5 inhibitor PF-4540124, *Mol. BioSyst.*, 2009, **5**, 472–482.

45 S. F. Steinberg and L. L. Brunton, Compartmentation of G protein-coupled signaling pathways in cardiac myocytes, *Annu. Rev. Pharmacol. Toxicol.*, 2001, **41**, 751–773.

46 M. Zaccolo and M. A. Movsesian, cAMP and cGMP signaling cross-talk: role of phosphodiesterases and implications for cardiac pathophysiology, *Circ. Res.*, 2007, **100**, 1569–1578.

47 S. Resjö, A. Oknianska, S. Zolnierowicz, V. Manganiello and E. Degerman, Phosphorylation and activation of phosphodiesterase type 3B (PDE3B) in adipocytes in response to serine/threonine phosphatase inhibitors: deactivation of PDE3B *in vitro* by protein phosphatase type 2A, *Biochem. J.*, 1999, **341**(pt 3), 839–845.
48 D. M. Virshup, Protein phosphatase 2A: a panoply of enzymes, *Curr. Opin. Cell Biol.*, 2000, **12**, 180–185.
49 K. Lechward, O. S. Awotunde, W. Swiatek and G. Muszyńska, Protein phosphatase 2A: variety of forms and diversity of functions, *Acta Biochim. Pol.*, 2001, **48**, 921–933.
50 V. Janssens, J. Goris and C. Van Hoof, PP2A: the expected tumor suppressor, *Curr. Opin. Genet. Dev.*, 2005, **15**, 34–41.
51 T. Glatter, A. Wepf, R. Aebersold and M. Gstaiger, An integrated workflow for charting the human interaction proteome: insights into the PP2A system, *Mol. Syst. Biol.*, 2009, **5**, 237.
52 A. Shevchenko, O. N. Jensen, A. V Podtelejnikov, F. Sagliocco, M. Wilm, O. Vorm, P. Mortensen, H. Boucherie and M. Mann, Linking genome and proteome by mass spectrometry: large-scale identification of yeast proteins from two dimensional gels, *Proc. Natl. Acad. Sci. U. S. A.*, 1996, **93**, 14440–14445.
53 C. K. Frese, A. F. Altelaar, M. L. Hennrich, D. Nolting, M. Zeller, J. Griep-Raming, A. J. Heck and S. Mohammed, Improved peptide identification by targeted fragmentation using CID, HCD and ETD on an LTQ-Orbitrap Velos, *J. Proteome Res.*, 2011, **10**, 2377–2388.
54 E. Corradini, R. Vallur, L. M. Raaijmakers, S. Feil, R. Feil, A. J. R. Heck and A. Scholten, Alterations in the cerebellar (Phospho)proteome of a cyclic guanosine monophosphate (cGMP)-dependent protein kinase knockout mouse, *Mol. Cell. Proteomics*, 2014, **13**, 2004–2016.
55 J. A. Vizcaino, R. G. Cote, A. Csordas, J. A. Dianes, A. Fabregat, J. M. Foster, J. Griss, E. Alpi, M. Birim, J. Contell, G. O'Kelly, A. Schoenegger, D. Ovelleiro, Y. Perez-Riverol, F. Reisinger, D. Rios, R. Wang and H. Hermjakob, The PRoteomics IDEntifications (PRIDE) database and associated tools: status in 2013, *Nucleic Acids Res.*, 2013, **41**, D1063–D1069.